OPTICAL FIBRES

PACS numbers: 42.81.– i; 42.79.Dj
DOI: 10.1070/QE2006v036n01ABEH013045

Modification of cladding-mode fields upon fibre loading with H_2 and its influence on the spectral characteristics of long-period gratings

S.A. Vasil'ev, O.I. Medvedkov, A.S. Bozhkov, I.G. Korolev, E.M. Dianov

***Abstract*. The influence of diffusion of molecular hydrogen used to write fibre gratings on the spectral characteristics of the gratings is discussed in detail. It is shown that the additional waveguide structure formed by the concentration profile of dissolved molecular hydrogen modifies the spatial distribution of the field of fibre cladding modes, resulting in a considerable change in the coupling coefficient of long-period gratings. This modification is manifested most strongly for cladding modes with low radial indices.**

Keywords: *optical fibre, long-period fibre grating, cladding modes.*

1. Introduction

Photoindiced fibre gratings, both fibre Bragg gratings (FBGs) and long-period fibre gratings (LPFGs) are widely used at present in fibreoptic systems as spectrally selective elements [1, 2]. The most popular technique for producing such gratings in doped silica fibres is the induction of the refractive index in the fibre core by exposing it to intense UV radiation. There exist various grating writing schemes and their choice is determined by the required spectral properties of the gratings [1, 2].

To enhance the photosensitivity of the most widespread germanosilicate fibres, which is often insufficient for practical applications, the low-temperature ($T < 100$ °C) loading of fibres with molecular hydrogen in a chamber at a pressure of 100 – 200 atm is used, as a rule [3]. As a result, molecular hydrogen enters into a glass matrix in a physically dissolved state, not forming chemical bonds with a regular glass matrix and defect centres. A complete loading of a standard fibre of diameter 125 μm at room temperature can be achieved for about two weeks. The loading time can be considerably reduced (down to 10 – 12 hours) by increasing temperature up to 80 – 100 °C; however, the resulting concentration of H_2 in the glass matrix noticeably decreases in this case [4].

During grating fabrication, the dissolved molecular hydrogen interacts with defect centres and regular bonds of the germanosilicate glass network by forming hydrogen groups and catalyses other photoinduced processes resulting in a permanent change in the refractive index of the glass [5, 6]. The hydrogen loading provides the increase in the UV radiation induced refractive index up to 10^{-2}, which is approximately an order of magnitude higher than the values achieved in fibres without hydrogen loading. After grating production, fibres are kept at a temperature of 20 – 100 °C for a certain time to allow molecular hydrogen, which did not enter into the reaction, to leave the fibre.

The use of hydrogen in grating production involves, along with the advantages considered above, a number of difficulties because hydrogen at such a high molar concentration (a few percent) noticeably changes the refractive index of silica glass (by 10^{-3} and more [4, 7]). Therefore, the H_2 concentration and its spatial distribution should be taken into account in the production of gratings with the required spectral properties, i.e., diffusion processes should be considered both between different regions inside the fibre and between the fibre and environment, which proceed during grating fabrication and after it.

In this paper, we studied for the first time the influence of the spatial distribution of the concentration of molecular hydrogen on the distribution of the field of fibre cladding modes and the intermode interaction intensity in LPFGs.

2. Characteristic diffusion times affecting the properties of fibre gratings

The writing dynamics of fibre-grating spectral properties can be described by several characteristic times, which are related to the dimensions of fibre regions where hydrogen diffusion occurs. Figure 1 presents the dependence of the characteristic diffusion time τ (the time during which the hydrogen concentration C_{H_2} in the fibre becomes equal to half the maximum achievable concentration $C_{H_2}^{max}$) on the diameter of the region to which or out of which the diffusion of H_2 occurs at room temperature. The calculation was performed for a silica cylinder by using the diffusion coefficient $D_{H_2}(25\,^\circ\mathrm{C}) = 2.5\times\ 10^{-11}$ cm^2 s^{-1} [8]. The dashed straight lines indicate the diffusion times observed in gratings written in a standard fibre with the core diameter $d_{core} = 9$ μm and the cladding diameter $d_{clad} = 125$ μm.

In particular, diffusion occurs most rapidly over distances of the order of the FBG period $\Lambda_{BG} \sim 0.5$ μm and has the characteristic time $\tau_{BG} \sim 5$ s. This diffusion occurs from a non-irradiated region of the fibre core to an irradiated region, where the concentration of H_2 decreased

S.A. Vasil'ev, O.I. Medvedkov, A.S. Bozhkov, I.G. Korolev, E.M. Dianov Fiber Optics Research Center, A.M. Prokhorov General Physics Institute, Russian Academy of Sciences, ul. Vavilova 38, 119991 Moscow, Russia; e-mail: sav@fo.gpi.ru

Received 19 September 2005
Kvantovaya Elektronika **36** (1) 61 – 66 (2006)
Translated by M.N. Sapozhnikov

due to its interaction with the glass matrix, and is manifested in a weak increase in the reflection coefficient of a FBG. This process is rarely observed in a pure form because the typical writing time of gratings (several minutes) considerably exceeds τ_{BG}. Note that such diffusion does not play a noticeable role in LPFGs due to a relatively long period of these gratings.

Diffusion of H_2 from a silica cladding to the fibre core hydrogen-depleted after irradiation affects the spectral properties of gratings of both types. For standard fibres with $d_{core} = 9$ μm, the characteristic time τ_{core} of this diffusion at room temperature is ~ 30 min (Fig. 1). Such a diffusion process, by increasing the effective refractive index for the fundamental mode of the fibre, results in the red shift of the resonance wavelength of a FBG, which typically does not exceed 0.1 – 0.2 nm [9]. The value of this shift in LPFGs is difficult to determine due to the simultaneous diffusion of H_2 from the fibre to the environment, which also causes the red shift of the resonance wavelength in the above-mentioned time range. Note that during the H_2 diffusion from the fibre cladding to its core, the coupling coefficient of gratings increases because a greater amount of hydrogen diffuse into the irradiated region of the fibre core for the reasons presented above [10 – 12].

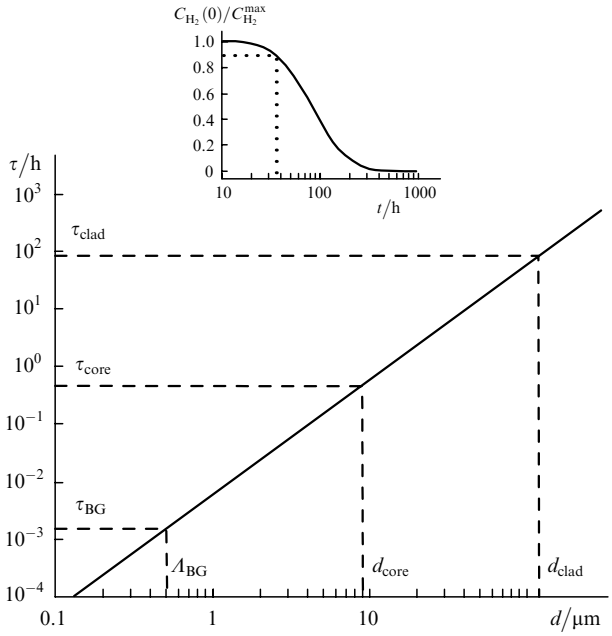

Figure 1. Dependence of the characteristic diffusion time τ of molecular hydrogen on the silica-cylinder diameter d at room temperature. The insert shows the dependence of the relative hydrogen concentration on the axis of the fibre of diameter 125 μm on the time after its hydrogen loading.

The influence of the molecular hydrogen diffusion from a fibre to the environment on the spectral properties of gratings (grating spectra), which is the longest process among all the processes studied, was investigated in detail in the literature. The characteristic time τ_{clad} of this process for a standard fibre is ~ 100 h (Fig. 1). This process is manifested in FBG spectra mainly in the blue shift of the resonance wavelength by no more than 1 nm [9]. Variations observed in LPFG spectra are more complicated [13, 14]. First the resonance wavelength increases, which corresponds to a decrease in the effective refractive index for cladding modes during hydrogen diffusion from the fibre cladding. Only when the hydrogen concentration on the fibre axis begins to decrease (see insert in Fig. 1), the effective refractive index for the fundamental mode decreases, which in turn reduces the resonance wavelength of the LPFG. Note that this wavelength dynamics is typical for the normal LPFG resonances, whereas for anomalous resonances [15] opposite shifts are typical.

The strength of action of diffusion processes on the spectral properties of fibre gratings can vary in a broad range because the intensity of these processes strongly depends on the writing parameters of gratings, the initial H_2 concentration and its distribution in the fibre, the fibre temperature, and other factors.

Below, we consider in detail another phenomenon, which, in our opinion, has not been discussed in the literature so far and should be taken into account in the analysis of diffusion processes proceeding during fibre grating fabrication. We found that the diffusion of H_2 from a fibre causes not only the shift of the resonance wavelength of a LPFG but also considerable changes the resonance depth, the value of this change being substantially dependent on the number of an excited cladding mode. The maximum change in the resonance depth is observed when the H_2 concentration on the fibre axis begins to decrease, i.e., at room temperature within 30 – 40 h after the end of hydrogen loading of the fibre (dotted straight line in the insert in Fig. 1).

3. Experimental

In our experiments, we tried to separate the effect under study from other diffusion processes. For this purpose, fibres with preliminary written LPFGs were subjected to hydrogen loading. Before loading, the gratings were additionally annealed to provide the invariable distribution of the UV radiation induced refractive index during subsequent studies.

Gratings were written step-by-step in a standard SMF-28 fibre by the 244-nm second harmonic radiation from an argon laser [16]. The writing power density was 10 kW cm^{-2} and the integrated dose was 5 kJ cm^{-2}. The photosensitivity of fibres was enhanced before LPFG writing by loading them with hydrogen at a pressure of 125 atm and temperature 100 °C up to the molar concentration of $H_2 \sim 1.1$ % in the glass matrix [7]. The fibre gratings had a period of 450 μm and a length of 400 mm. After grating writing and escape of the residual hydrogen from the fibre, the gratings were annealed in a resistive furnace at a temperature of 500 °C for 15 min.

The LPFGs prepared in this way were again loaded with hydrogen with the parameters presented above. The H_2 escape was studied immediately after loading by using an automated setup for a linear heating of fibres [17] with a heating rate of 0.05 °C s^{-1} in the temperature range from 25 to 300 °C. This measuring procedure was repeated after complete cooling of the furnace to determine a change in the properties of gratings in the absence of dissolved H_2 in the fibre. The transmission spectra of LPFGs were measured during heating every 20 s. Note that the method of linear heating considerably reduces the measurement time compared to that at room temperature, thereby improving the measurement accuracy.

4. Results and discussion

The dynamics of spectral characteristics of a LPFG is illustrated in Fig. 2 where the transmission spectra of the grating measured at different temperatures during linear heating are presented. The spectral shift of the resonance peaks is indicated schematically by the arrows. In the spectral range under study and the grating parameters indicated above, the fundamental HE_{11} mode of the fibre is resonantly coupled with the $HE_{12} - HE_{15}$ cladding modes. The maximum shift of the resonance peaks of the LPFG was observed at 170 °C [curve (*2*)]. The depth of the resonance peaks in the reflection spectrum of the LPFG achieved its maximum also at these temperatures.

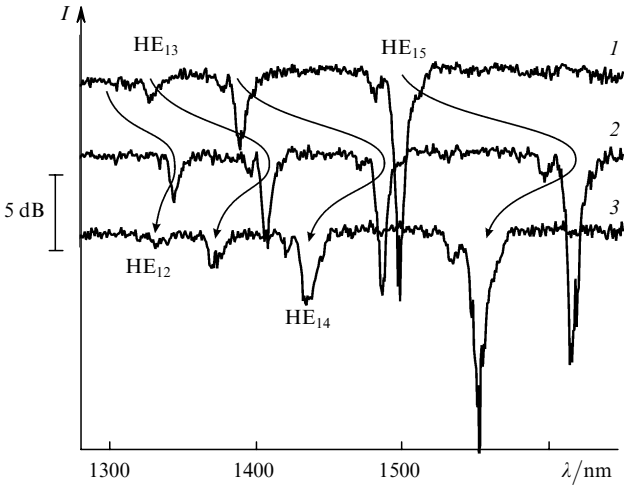

Figure 2. Transmission spectra of the LPFG after loading the fibre with hydrogen at temperatures 25 (*1*), 170 (*2*), and 300 °C (*3*) measured during linear heating.

A convenient characteristic of the peak depth is the product of the grating coupling coefficient κ by the grating length L, which is related with the peak depth S by the expression $\kappa L = \arcsin\sqrt{S}$ [18]. Figure 3 presents the temperature dependences of the product κL and resonance wavelengths λ^{res} obtained for four LPFG peaks after hydrogen loading and in the absence of hydrogen in the glass matrix.

Let us call attention to a number of circumstances following from Figs 2 and 3. After hydrogen loading of fibres, the resonance peaks of the LPFG shifted to the blue ($\Delta\lambda^{res}_{H_2}$ in Fig. 3b). In addition, the depth of resonances somewhat decreased [$\Delta(\kappa L)_{H_2}$ in Fig. 3a]. The nature of these changes is not clear at present and requires further studies. It seems that they can be caused by different degrees of H_2 solubility in different regions of the fibre.

Figure 3b clearly demonstrates the nonmonotonic dynamics of the shift of resonance wavelengths, which is typical for LPFGs during the escape of hydrogen from the fibre [13]. In addition, the depth of resonance peaks for the lowest cladding modes considerably changes, the relative value of this change decreasing with increasing the mode index. Note that the temperature at which the maximum shift of λ^{res} occurs is the same for all the LPFG peaks (~170 °C), whereas the value of κL for different resonances achieves a maximum at different temperatures in the range 130 – 170 °C (Fig. 3a).

Note that the coupling coefficient in the LPFG not loaded with hydrogen (dashed curves in Fig. 3a) does not change in fact during heating, which points to the absence of a temperature-reversible change in the induced refractive index studied in [19] and well agrees with the results of this paper. The monotonic increase in λ^{res} for this grating upon heating characterises the temperature sensitivity of the resonance peaks, which increases with increasing the cladding mode number [20, 21]. The fact that the solid and dashed curves in Fig. 3b coincide at temperatures above 250 °C means that H_2 completely escaped from the fibre at such temperatures.

To explain a change in the depth of LPFG resonances, we consider the dynamics of the H_2 escape from the fibre. Figure 4 presents the radial distributions of the relative concentration of H_2 calculated for the heating parameters indicated above. We used in the calculation the temperature dependence of the diffusion coefficient of molecular hydrogen in a silica glass, which well agrees with the experimental data obtained in many papers:

$$D_{H_2} = 2.83 \times 10^{-4} \exp\left(-\frac{40.19\ \text{kJ mol}^{-1}}{RT}\right), \qquad (1)$$

where R is the universal gas constant [8] and D_{H_2} has the dimensionality cm ^{2} s^{-1}. We also assumed that the initial concentration of hydrogen $C^{max}_{H_2}$ was constant along the fibre radius, i.e., the solubility degree of H_2 was the same in

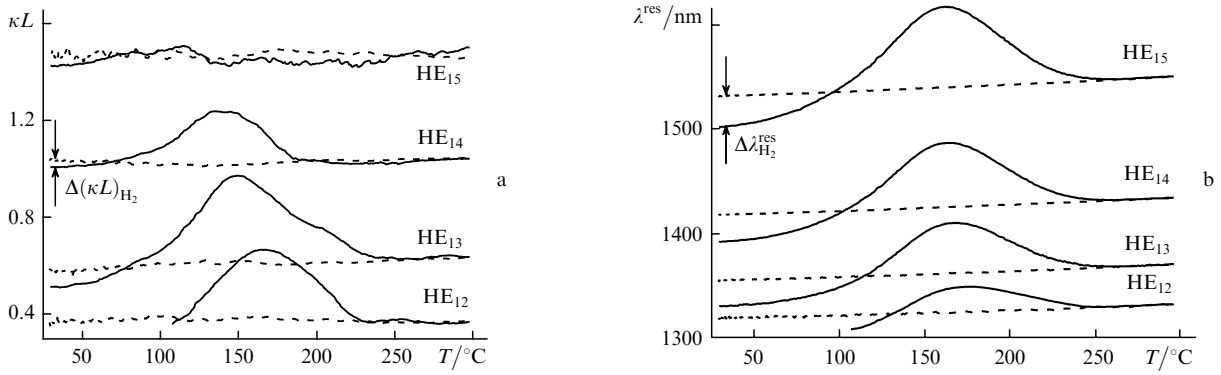

Figure 3. Temperature dependences of κL (a) and the resonance wavelengths λ^{res} (b) of the LPFG upon linear heating of the grating in the hydrogen-loaded fibre (solid curves) and in the absence of hydrogen in the glass matrix (dashed curves) for different modes.

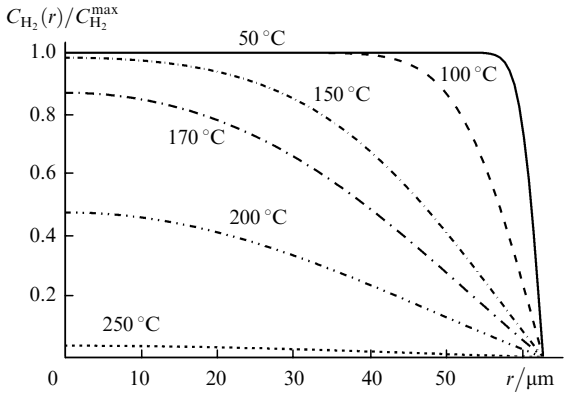

Figure 4. Radial distributions of the relative H_2 concentration calculated for a linear heating of a standard fibre at a rate of 0.05 °C s^{-1}.

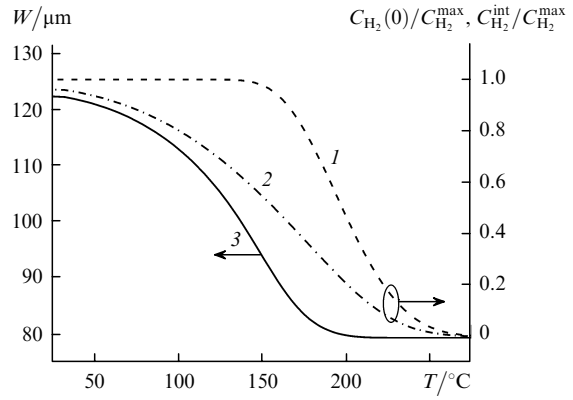

Figure 5. Temperature dependences of the relative H_2 concentration on the fibre axis (*1*), the relative integral H_2 concentration in the fibre (*2*), and the FWHM W of the spatial distribution of the H_2 concentration (*3*) calculated for linear heating of a standard fibre at a rate of 0.05 °C s^{-1}.

the fibre volume. One can see that, under our experimental conditions up to temperature ~ 150 °C, hydrogen mainly escapes from the fibre cladding, and only when temperature is further increased, the hydrogen concentration in the fibre core decreases.

As mentioned above, the refractive index of a silica glass increases proportionally to the concentration of hydrogen dissolved in it, so that the distributions shown in Fig. 4 are in fact the additional graded-index waveguide structure produced by hydrogen dissolved in the fibre. Such a hydrogen-induced waveguide structure can not only change the efficient refractive index of a mode but also modify the distributions of mode fields.

Figure 5 shows the calculated temperature dependences of a number of parameters obtained in the linear heating regime. Note that curves (*1*) and (*2*) in Fig. 5 characterise hydrogen-induced variations in the effective refractive indices for fibre modes. Indeed, a change in the effective refractive index of the fundamental mode of the fibre is proportional to the molar concentration of H_2 on the fibre axis: $\delta n_{eff}^{core} \approx \alpha_{H_2} C_{H_2}(0)$, where $\alpha_{H_2} = dn/dC_{H_2} = 4.42 \times 10^{-4}$ inverse percent [7]. At the same time, assuming that the amplitude of the cladding-mode field is constant along the fibre radius, we obtain that a change in the effective refractive index of cladding modes is proportional to the integral concentration of H_2 in the fibre with the same proportionality coefficient: $\delta n_{eff}^{clad} \approx \alpha_{H_2} C_{H_2}^{int}$.

Figure 6 presents the radial field distributions for the lowest and highest cladding modes studied by us, which were calculated for several temperatures, i.e., for the H_2 concentration distributions corresponding to these temperatures (Fig. 4). The hydrogen-induced variations are most strong for the first cladding mode and decrease with increasing the radial mode index, the maximum changes in the distributions for all cladding modes being observed in the temperature region from 150 to 170 °C. As shown in Fig. 5, at such temperatures the hydrogen-induced refractive index has the maximum amplitude and the minimum width.

The coupling coefficient of the LPFG increases mainly due to a considerable increase in the amplitude of the cladding-mode field in the fibre core (Fig. 6a) and the corresponding increase in the overlap integral between cladding and core modes [18]. All these facts are in good agreement with the experimental results presented above (Fig. 3).

Figure 7 shows the experimental [curves (*1*)] and calculated [curves (*2*)] temperature dependences of the quantity κL and the wavelength shift $\delta\lambda^{res}$ for the resonance corresponding to the $HE_{11} - HE_{12}$ mode coupling. The spectral characteristics of the LPFG were calculated by the method described in [18]. The experimental and calculated temperature dependences of κL well coincide both in their positions and maxima (Fig. 7a). The positions of maxima of the experimental and calculated dependences $\delta\lambda^{res}(T)$ in Fig. 7b are in good agreement. Note that curve

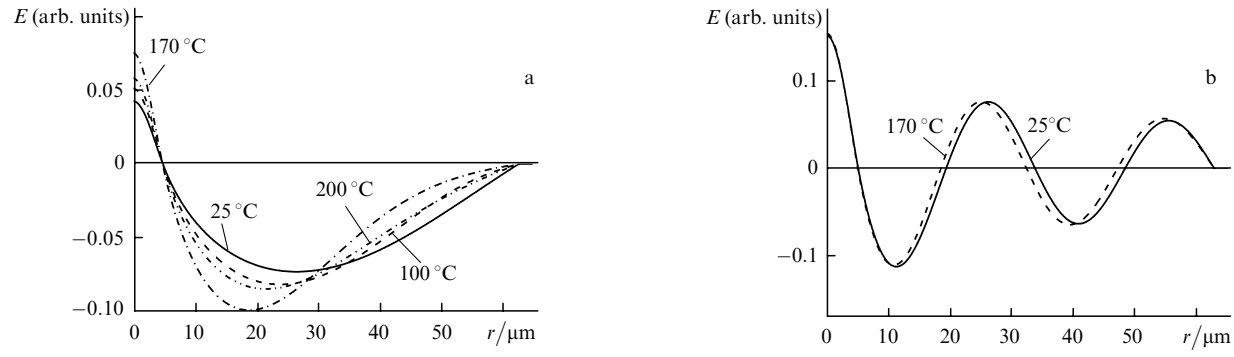

Figure 6. Radial distributions of the fields E of cladding modes HE_{12} (a) and HE_{15} (b) calculated at different temperatures upon linear heating of the LPFG in the hydrogen-loaded fibre.

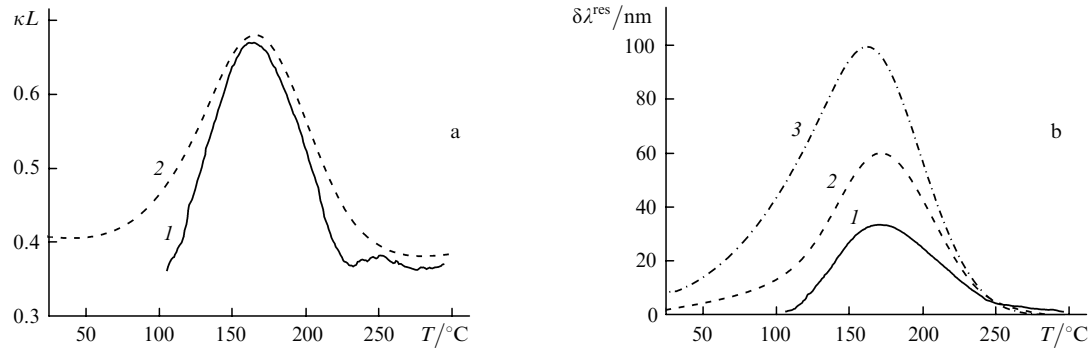

Figure 7. Experimental (*1*) and calculated (*2*, *3*) temperature dependences of κL (a) and the resonance wavelength shift $\delta\lambda^{res}$ (b) for the peak corresponding to the $HE_{11} - HE_{12}$ mode coupling for a linearly heated fibre. Curve (*3*) is calculated by (2).

(*1*) in Fig. 7b was corrected taking into account the temperature sensitivity of the peak and the hydrogen-induced initial wavelength shift $\Delta\lambda^{res}_{H_2}$ (Fig. 3b). The differences between the absolute values of $\delta\lambda^{res}$ obtained in the experiment and calculations (Fig. 7b) are probably explained by the fact that we have failed to take accurately into account the dispersion characteristics of fibre modes.

The dynamics of the resonance wavelength can be approximately estimated by using the phase-matching condition for the LPFG modes [18]: $\lambda^{res} = (n^{core}_{eff} - n^{clad}_{eff})\Lambda$, where Λ is the LPFG period. By assuming that the difference of the effective refractive indices of the fibre modes is independent of the wavelength (this dependence should be taken into account in the general case [22]) and using the relations obtained above, we can represent the expression for the hydrogen-induced change in λ^{res} in the form

$$\delta\lambda^{res} = (\delta n^{core}_{eff} - \delta n^{clad}_{eff})\Lambda \approx \alpha_{H_2}[C_{H_2}(0) - C^{int}_{H_2}]\Lambda. \qquad (2)$$

Curve (*3*) in Fig. 7b was calculated by expression (2). One can see that it qualitatively correctly describes the experiment and can be used for approximate estimates. It is important that this approximate dependence can be used for any cladding mode and it was obtained without solving the wave equation.

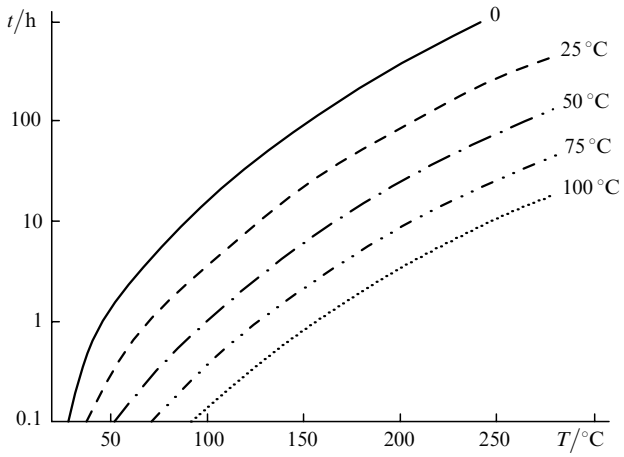

Figure 8. Temperature dependences of the hold time of the fibre in the isothermal regime on the temperature upon linear heating at a rate of $0.05\,^{\circ}C\ s^{-1}$.

Note that a change in the H_2 concentration profile and the related change in the amplitude of the LPFG peaks occur at any LPFG storage and annealing regimes. It is interesting from the practical point of view to study the dynamics of the LPFG spectrum at room temperature. To compare the results that we obtained during linear heating with the isothermal regime of gratings, we present in Fig. 8 the calculated dependences of the hold time of the fibre at constant temperature on temperature upon heating the fibre at a rate of $0.05\,^{\circ}C\ s^{-1}$. For example, for temperature 170 °C, at which the maximum depth of the $HE_{11} - HE_{12}$ mode is observed, the hold time is ~ 40 h at temperature 25 °C and ~ 1.5 h at temperature 100 °C.

5. Conclusions

The experimental and calculated dependences presented in the paper have clearly shown that the depth of the resonance peaks of long-period gratings changes after the diffusion of hydrogen from the fibre due to the change in the overlap integral for cladding and core modes of the fibre. The overlap integral changes due to the modification of the cladding mode fields caused by the change in the concentration profile of molecular hydrogen dissolved in the fibre. This effect is especially distinct for the resonances caused by the coupling of the fundamental mode with modes with low radial indices.

Thus, the molecular hydrogen dissolved in a fibre produces an additional waveguide structure whose properties change according to the change in the concentration profile of hydrogen and which should be taken into account during fibre grating production.

This interpretation improves the understanding of the complicated dynamics of spectral characteristics of LPFGs observed during the hydrogen diffusion from the fibre. In addition, it also allows one to take into account the conditions of fibre storage after loading with hydrogen during the formation of gratings with specified spectral characteristics. The effect considered in the paper can be used for diagnostics of the current distribution of hydrogen dissolved in fibres.

Note in conclusion that the results obtained for the diffusion of molecular hydrogen can be also applied, by using the corresponding diffusion coefficient and solubility, to molecular deuterium, which, as molecular hydrogen, is widely used to enhance the photosensitivity of fibres [23].

Acknowledgements. This work was partially supported by the Russian Foundation for Basic Research (Grant No 04-02-17025) and the Moscow Committee on Science and Technologies (Grant No 1.2.2, 2005).

References

1. Kashyap R. *Fiber Bragg Gratings* (San Diego, London: Acad. Press, 1999).
2. Othonos A., Kalli K. *Fiber Bragg Gratings: Fundamentals and Applications in Telecommunications and Sensing* (Norwood, Mass.: Artech House, 1999).
3. Lemaire P.J., Atkins R.M., Mizrahi V., Reed W.A. *Electron. Lett.*, **29**, 1191 (1993).
4. Swart P.L., Chtcherbakov A.A. *J. Lightwave Technol.*, **20**, 1933 (2002).
5. Tsai T.-E., Williams G.M., Friebele E.J. *Opt. Lett.*, **22**, 224 (1997).
6. Cordier P., Dalle C., Depecker C., Bernage P., Douay M., Niay P., Bayon J.-F., Dong L. *J. Non-Cryst. Solids*, **224**, 277 (1998).
7. Vasil'ev S.A., Rybaltovskii A.O., Koltashev V.V., Sokolov V.O., Klyamkin S.N., Medvedkov A.I., Ryabaltovskii A.A., Malosiev A.R., Plotnichenko V.G., Dianov E.M. *Kvantovaya Elektron.*, **35**, 278 (2005) [*Quantum Electron.*, **35**, 278 (2005)].
8. Lemaire P.J. *Opt. Eng.*, **30**, 780 (1991).
9. Malo B., Albert J., Hill K.O., Bilodeau F., Johnson D.C. *Electron. Lett.*, **30**, 442 (1994).
10. Guan B.O., Tam H.Y., Ho S.L., Liu S.Y., Dong X.Y. *IEEE Photon. Techn. Lett.*, **12**, 642 (2000).
11. Guan B., Tam H., Chan H., Choy C., Demokan M.S. *Meas. Sci. Technol.*, **12**, 818 (2001).
12. Mizunami T., Fukuda T., Hayashi A. *Meas. Sci. Technol.*, **15**, 1467 (2004).
13. Bhakti F., Larrey J., Sansonetti P., Poumellec B. *Proc. Bragg Gratings, Photosensitivity, and Poling in Glass Waveguides Conf.* (Washington, DC: OSA, 1997) BSuD4, p. 55.
14. Jang J.N., Kwack K.H. *Proc. Bragg Gratings, Photosensitivity, and Poling in Glass Waveguides Conf.* (Washington, DC: OSA, 1997) BMG10, p. 213.
15. Shu X., Zhang L., Bennion I. *J. Lightwave Technol.*, **20**, 255 (2002).
16. Dianov E.M., Vasil'ev S.A., Starodubov D.S., Frolov A.A., Medvedkov O.I. *Kvantovaya Elektron.*, **24**, 160 (1997) [*Quantum Electron.*, **27**, 155 (1997)].
17. Bozhkov A.S., Vasil'ev S.A., Medvedkov A.I., Grekov M.V., Korolev I.G. *Prib. Tekhn. Eksp.*, **48**, 491 (2005).
18. Vasil'ev S.A., Dianov E.M., Kurkov A.S., Medvedkov O.I., Protopopov V.N. *Kvantovaya Elektron.*, **24**, 151 (1997) [*Quantum Electron.*, **27**, 146 (1997)].
19. Hidayat A., Wang Q., Niay P., Douay M., Poumellec B., Kherbouche F., Riant I. *Appl. Opt.*, **40**, 2632 (2001).
20. Dianov E.M., Kurkov A.S., Medvedkov O.I., Vasiliev S.A. *Proc. X Eurosensors European Conf. on Solid-State Transducers* (Leuven, Belgium, 1996) P5.1–128.
21. Bhatia V., Vengsarkar A.M. *Opt. Lett.*, **21**, 692 (1996).
22. Erdogan T., Stegall D. *Proc. Optical Fiber Communication Conf.* (Washington, DC: OSA, 1998) ThG5, p. 280.
23. Mizrahi V., Lemaire P.J., Erdogan T., Reed W.A., DiGiovanni D.J. *Appl. Phys. Lett.*, **63**, 1727 (1993).